

# Towards quantum thermodynamics in electronic circuits

Jukka P. Pekola

**Electronic circuits operating at sub-kelvin temperatures are attractive candidates for studying classical and quantum thermodynamics: their temperature can be controlled and measured locally with exquisite precision, and they allow experiments with large statistical samples. The availability and rapid development of devices such as quantum dots, single-electron boxes and superconducting qubits only enhance their appeal. But although these systems provide fertile ground for studying heat transport, entropy production and work in the context of quantum mechanics, the field remains in its infancy experimentally. Here, we review some recent experiments on quantum heat transport, fluctuation relations and implementations of Maxwell’s demon, revealing the rich physics yet to be fully probed in these systems.**

Thermodynamics and statistical physics have attracted renewed interest in recent years, largely owing to an improvement in the experimental control of small structures, all the way down to the nanoscale. Phenomena on these scales can be described using stochastic thermodynamics<sup>1</sup>, which includes the influence of fluctuations inherent in such small systems, and applies to non-equilibrium processes far beyond the linear response regime. Until recently, experiments on molecules and soft matter at ambient temperatures have dominated the field<sup>2,3</sup>. But such experiments cannot be easily extended into the quantum regime, which presents an exciting frontier in this area of research. Electrical circuits at low temperatures, on the other hand, are suitable for thermodynamic studies in both classical and quantum regimes. The ‘quantumness’ of these circuits has been widely demonstrated over the past decade by the vigorous activity on the coherent properties of both superconducting and semiconducting qubits at low temperatures.

## Dissipation and entropy production in electronic circuits

Electrons in a metal form a Fermi distribution in equilibrium with a phonon bath. These electrons can easily be driven out of equilibrium, for example, by applying Joule heating<sup>4</sup>. A key feature of these circuits, which operate at sub-kelvin temperatures, is a striking separation of timescales, together with the possibility of controlling them. For example, relaxation between electrons and phonons at low temperatures is orders of magnitude slower than their internal relaxation rates. This means that subsystems with differing but well-defined temperatures can exist within the same system. The phonon system is typically assumed to be the ‘true’ bath, with constant temperature provided by the macroscopic thermostat (or cryostat). Adapting this typical scenario can give rise to an ideal platform from which to study the statistical physics and thermodynamics of nanostructures at sub-kelvin temperatures (Fig. 1a).

A biased tunnel barrier between two conductors with a chemical potential difference of  $\Delta\mu = eV$ , where  $e$  is the electronic charge and  $V$  is the voltage drop (Fig. 1b,c), forms the basic unit for studies of fluctuations and non-equilibrium physics in a circuit. Consider a single tunnelling event, depicted in the figure as the creation of a hole-like and particle-like excitation in the left and right leads, respectively. For this event, the transition rate  $\Gamma$  is determined by the

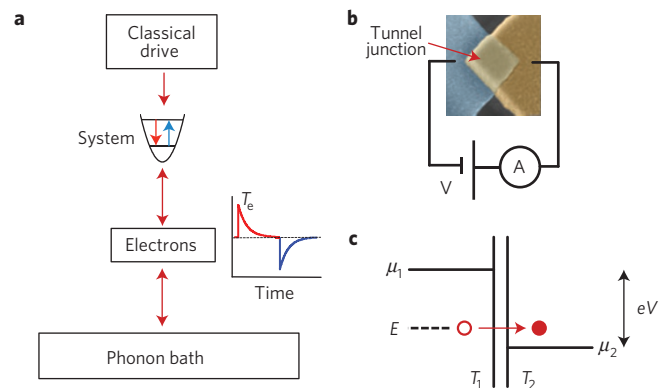


**Figure 1 | Dissipation and relaxation in electronic circuits at low temperatures.** **a**, A generic thermal model. A system, for example, a charge state in a single-electron experiment or qubit, is driven by a source of work. The system interacts with the Fermi-distributed electrons, which, in turn, tend to thermalize with the bath of phonons through electron-phonon coupling. The state of the system and/or the temperature of the electrons  $T_e$  are measured in real time. **b**, A biased tunnel junction, formed of two metal leads to the left and right of the overlap area where the two conductors are attached by an oxide barrier. **c**, Dissipation in a tunnelling event through a barrier. An excitation is created on both sides of the barrier.

barrier itself,  $\Delta\mu$ , together with the temperatures  $T_1, T_2$  of the leads, and the type and density of the carriers. Tunnelling is a stochastic Poisson process, which obeys the principle of detailed balance,  $\Gamma(-\Delta\mu) = e^{-\Delta\mu/k_B T} \Gamma(\Delta\mu)$ , with  $k_B$  the Boltzmann constant, for equilibrium leads ( $T_1 = T_2 = T$ ). For a tunnelling electron with energy  $E$ , the energy deposition to the source lead is given by  $\Delta E_1 = \mu_1 - E$  and the entropy production is  $\Delta S_1 = (\mu_1 - E)/T_1$ , where  $\mu_1$  is the chemical potential of the lead. Correspondingly, for the drain lead, we have an energy deposition of  $\Delta E_2 = E - \mu_2$  and an entropy production of  $\Delta S_2 = (E - \mu_2)/T_2$ . In general, the total energy dissipation in this event is thus  $\Delta E = \Delta E_1 + \Delta E_2 = \mu_1 - \mu_2 = eV$ , determined by the chemical potential difference only.

If fluctuations are ignored, and there are tunnelling events occurring at an average rate of  $f = I/e$ , where  $I$  is the mean

Low Temperature Laboratory, Department of Applied Physics, Aalto University School of Science, PO Box 13500, 00076 Aalto, Finland. e-mail: jukka.pekola@aalto.fi

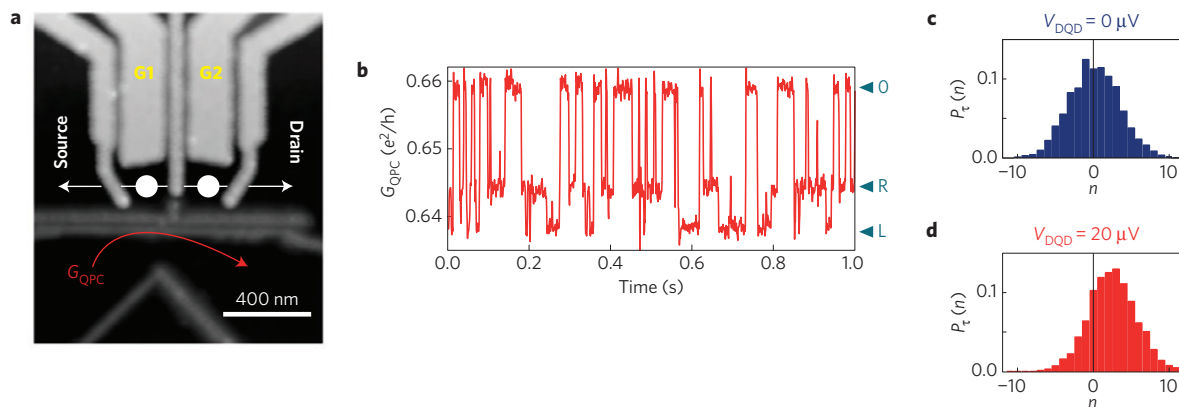


**Figure 2 | Testing the fluctuation theorem in equation (1) experimentally.** **a**, A double quantum-dot (DQD) circuit<sup>19</sup>. The physical positions of the dots for ( $n_1, n_2$ ) electrons between source and drain are indicated by white circles. A quantum point contact (QPC) reads the charge state on the left (L) or right (R) dot, or if both dots are empty (O). **b**, A time trace of the QPC conductance indicating whether there is an electron on the left (L) or right (R) dot, or if both dots are empty (O). **c,d**, Histograms of the net number  $n$  of charges that have passed from source to drain (**c**) at zero chemical potential difference and (**d**) at finite bias. The experiment is performed at  $T = 330$  mK.

electric current through the barrier, the average power dissipated is  $P = f \Delta E = IV$ . This result is quite general, independent of the type of the conductors at the junction. Although this total (average) power in a tunnel contact is positive, meaning there is net heating, one can engineer structures, for example, by applying materials with a gap in the density of states, where heat is distributed unequally between the two electrodes of the junction. In this way, evaporative cooling of electrodes can be achieved in both superconducting<sup>4,5</sup> and semiconducting<sup>6</sup> hybrid structures.

### Quantum heat transport

Let us first take a look at some experiments in which steady-state quantum heat transport has been investigated in a circuit. Based on information-theoretic arguments, John Pendry predicted in 1983 that a single quantum channel could conduct heat only up to a universal maximum value, determined by the quantum of thermal conductance  $G_Q = \pi k_B^2 T / (6\hbar)$  at temperature  $T$  (ref. 7), where  $\hbar$  is the Planck constant. Theoretical predictions of quantized thermal conductance for various types of carriers, phonons, photons and electrons were tested in nanostructures at sub-kelvin temperatures in the years following this claim. The development of nanosized circuits moved things forward, as the ability to create different local temperatures over nanoscale distances at low temperatures allowed precise measurements of the thermal conductance  $G_{th}$  of small conductors. In 2000, a beautiful experiment demonstrated that phonons in a nanobridge indeed carry heat at a rate of  $G_Q \Delta T$  per conduction channel, where  $\Delta T$  is the differential temperature bias around  $T$ , applied across the bridge<sup>8</sup>. The same effect was later seen in experiments in a superconducting circuit with two normal metal resistors interacting through thermal noise (or photons)<sup>9,10</sup>. A classical analogue of these experiments was recently implemented in a measurement with macroscopic resistors around room temperature, by detecting the thermal noise voltage across them<sup>11</sup>. In that experiment, the full distribution of heat transport was also measured. A recent experiment<sup>12</sup> provided a precision measurement of  $G_Q$  of electrons across a semiconducting quantum point contact. These measurements<sup>8–10,12</sup> demonstrate the power of hybrid micro- and nanocircuits at low temperatures as an arena for experiments on quantum thermodynamics and non-equilibrium thermal physics.

### Fluctuation relations

The importance of fluctuations in small systems with just a few degrees of freedom has also led to an upsurge of experimental and theoretical activity in the stochastic thermodynamics and

statistical mechanics of circuits. The classical version of the linear fluctuation–dissipation theorem (FDT) for heat current  $\dot{Q}$  is  $S_{\dot{Q}} = 2k_B T^2 G_{th}$ , in analogy with  $S_I = 2k_B T G$  for the noise of an electrical current  $I$  of a scatterer with conductance  $G$  (see, for example, ref. 13). Unlike that for the electrical current, the corresponding quantum version of the FDT for heat is still under debate<sup>14–16</sup>. More recently, non-equilibrium fluctuations far from equilibrium beyond the linear FDTs have attracted interest. The non-equilibrium fluctuation theorem<sup>1,17</sup> governing entropy  $S$  production can be cast generically in the form

$$P(\Delta S) / P(-\Delta S) = e^{\Delta S / k_B} \quad (1)$$

stating that the probabilities  $P$  for either increasing or decreasing the entropy by an amount  $\Delta S$  are related by this general equality in a given process. This relation leads to

$$\langle e^{-\Delta S / k_B} \rangle = 1 \quad (2)$$

by employing the definition  $\langle e^{-\Delta S / k_B} \rangle = \int d\Delta S P(\Delta S) e^{-\Delta S / k_B}$ . The expectation value  $\langle \cdot \rangle$  is to be understood as the average outcome of many repeated measurements, each under the same protocol.

Electrical circuits at low temperatures provide an interesting realization of non-equilibrium phenomena, and a well-controlled test bed for the fluctuations and dissipation that occur within them. The basic fluctuation theorem in equation (1) has been tested in experiments on a double quantum dot (DQD; refs 18,19). Although it is a quantum-dot structure, the experiment itself is in the classical single-electron tunnelling regime and thus probes the classical fluctuation relations. The set-up for this experiment is shown in Fig. 2. There are two dots between the source and drain leads at the left and right, respectively. The extra number of electrons on each dot, governed by the Coulomb energy of the small structure, is monitored by a quantum point contact (QPC). This QPC is asymmetrically coupled to the dots and therefore its electrical conductance is sensitive to the occupations ( $n_L, n_R$ ), where  $n_L$  ( $n_R$ ) is the number of extra electrons on the left (right) dot. At low enough temperatures, only three charge states are possible: (0, 0), (0, 1), (1, 0). The QPC can resolve between these three states, and can then be used to perform full counting statistics of charge—that is, to determine the full distribution of the number of charges traversed through the structure.

The drain–source voltage supply biased at voltage  $V_{DQD}$  does the work that leads to dissipation when  $n$  charges tunnel between these leads down in the potential. More precisely, the change of

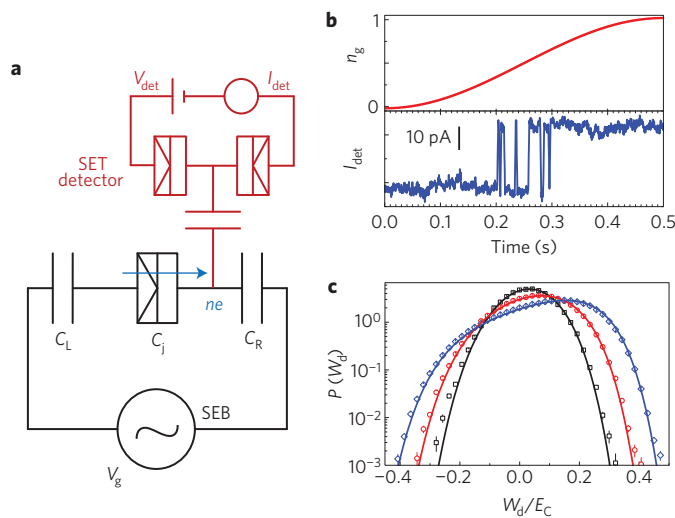


**Figure 3 | Experimental realization of the Jarzynski fluctuation relation.** **a**, A schematic diagram of a metallic single-electron box (SEB; ref. 29). The box is connected capacitively to its environment by  $C_L$  and  $C_R$ , and the two metallic electrodes are connected through a tunnel junction with capacitance  $C_j$ . The extra charge can dwell on either the left ( $n=0$ ) or the right ( $n=1$ ) island and the transition between the two states is indicated by the blue arrow. The current  $I_{det}$  of the voltage-biased single-electron transistor (SET) coupled capacitively to one of the islands of the SEB reads the charge state  $n$ . **b**, A time trace of the SET, where transitions between ( $n=0$ , lower value of  $I_{det}$ ) and ( $n=1$ , higher value of  $I_{det}$ ) are monitored in time and tagged with the driving field  $n_g \propto V_g$ . **c**, The distributions of dissipated work measured on the SEB at  $T=200$  mK at three different driving rates: 1 Hz (black), 2 Hz (red) and 4 Hz (blue). The solid lines are exact theoretical predictions using independently determined sample parameter values. The distributions become increasingly non-Gaussian with increasing rate. Each distribution is composed of more than  $10^5$  repetitions of the driving protocol. The Jarzynski equality  $\langle e^{-\beta W_d} \rangle = 1$ , where  $W_d \equiv W - \Delta F$ , is satisfied within 3% uncertainty for all three distributions.

entropy when  $n$  electrons ( $n$  can be positive or negative) tunnel from source to drain is  $neV_{DQD}/T$ , where  $T$  is now the common temperature of the two leads. For measuring times  $\tau$  that are long enough such that one can neglect the contribution of the internal charge state configuration on the dots at the beginning and the end of the experiment, one may then write equation (1) in the form  $P(n, \tau)/P(-n, \tau) = e^{neV_{DQD}/k_B T}$ . Under these fixed voltage bias conditions, the fluctuation relation then boils down to a measurement of electron counting statistics under detailed-balance conditions at temperature  $T$ .

These experiments serve as a beautiful demonstration of the principles of a fluctuation theorem in a well-characterized set-up. Yet the fluctuation theorem was not fully satisfied in this study (20–30% discrepancy in logarithmic ratio of the probabilities), owing to the measurement back-action and low bandwidth (‘slowness’) of the QPC detector<sup>20,21</sup>. Non-equilibrium (nonlinear) fluctuations of electrical current have also been highlighted in experiments on a semiconducting quantum conductor in the form of an Aharonov–Bohm ring<sup>22</sup>.

The non-equilibrium fluctuation relations can also be written for systems under time-dependent driving conditions. In this context, the work and, in particular, the so-called dissipated work become important concepts. A key fluctuation relation is then the Jarzynski equality<sup>23</sup> for a system coupled to a single heat bath, which takes a form similar to equation (2),

$$\langle e^{-\beta(W-\Delta F)} \rangle = 1 \tag{3}$$

Here  $\beta = (k_B T)^{-1}$  is the inverse temperature of the bath,  $W$  is the work done on the system of interest, and  $\Delta F$  is the change of its equilibrium free energy between the beginning and end points of the protocol. The Jarzynski equality is valid only for a system that is initially in thermal equilibrium with the bath, but it applies for driving protocols far from equilibrium. Comparing equations (2) and (3), we see that  $(W - \Delta F)/T$  is the entropy produced in the driven process. Based on elementary mathematical arguments, the equality implies that  $\langle W \rangle \geq \Delta F$ . That is, the second law of thermodynamics holds in the thermodynamic limit (in the sense of many realizations of the experiment). The counterpart of equation (1) for dissipated work in reversed protocols is called the Crooks relation<sup>24</sup>.

The practical importance of the Jarzynski equality is considered to be its ability to extract equilibrium properties of the system ( $\Delta F$ ) from non-equilibrium measurements. This quality has been harnessed in experiments on molecules and soft matter<sup>2,3</sup>. By contrast, the equilibrium properties of basic electronic circuits can generally be determined by other means, so the Jarzynski equality and the Crooks relation are superfluous to a large extent, as the relevant Hamiltonian including the coupling to the bath is typically known with high accuracy.

As a basic example, we consider a single-electron box (SEB; refs 25–28), which is tangentially related to the quantum-dot circuit discussed above. However, here we focus on a metallic system, where the only energy relevant for the system Hamiltonian is the Coulomb energy, and ‘particle-in-box’ quantum effects can be fully ignored. We are thus dealing with a system that is typically composed of about  $10^9$  free electrons. However, owing to the single-electron capacitive charging energy, the precise number of electrons in each conductor at a sufficiently low temperature is fixed at two possible values, say  $n=0$  and  $n=1$ . In the SEB drawn in Fig. 3, the total number of electrons on the two islands to the left and right of the tunnel junction in the middle (illustrated as a divided rectangle) is furthermore strictly constant, owing to the fact that each island is connected to the leads only with capacitors. The Hamiltonian of the box reads simply

$$H = E_C(n - n_g)^2 \tag{4}$$

Here  $E_C = e^2/(2C_\Sigma)$  is a constant for a particular box, determined by the total capacitance  $C_\Sigma$  of the SEB. The control parameter  $n_g$  is the source of work, and is proportional to the gate voltage  $V_g$  shown in Fig. 3.

A basic experiment on this type of system involves repeated ramps of the voltage from, say,  $n_g = 0$  to  $n_g = 1$  (ref. 29). The dissipation under non-equilibrium driving is associated with tunnelling events between the two islands that take place away from the energy degeneracy  $n_g = 1/2$ —that is, with non-zero  $\Delta\mu = 2E_C(n_g - 1/2)$ . Sweeps with the identical protocol—at an equal rate and over this same interval—are then measured to find the corresponding averages to test the Jarzynski equality and the Crooks relation. The entropy production and dissipated work, which in this case are equal (when the latter is divided by the bath temperature), are measured by a single-electron transistor (SET) that can detect the tunnelling events in the same way that the QPC can in the semiconductor circuits. Each tunnelling event is time-tagged to account for the instantaneous chemical potential difference, which is responsible for dissipation. In this way, this experiment goes beyond basic charge counting when measuring dissipation.

The results of this experiment satisfy the Jarzynski equality and the Crooks relation within about 3% uncertainty. Here, and in refs 18,19, it is worth noting that a large number of experiments is possible—up to millions of repetitions—meaning that sufficient statistics can be collected, unlike in typical experiments on

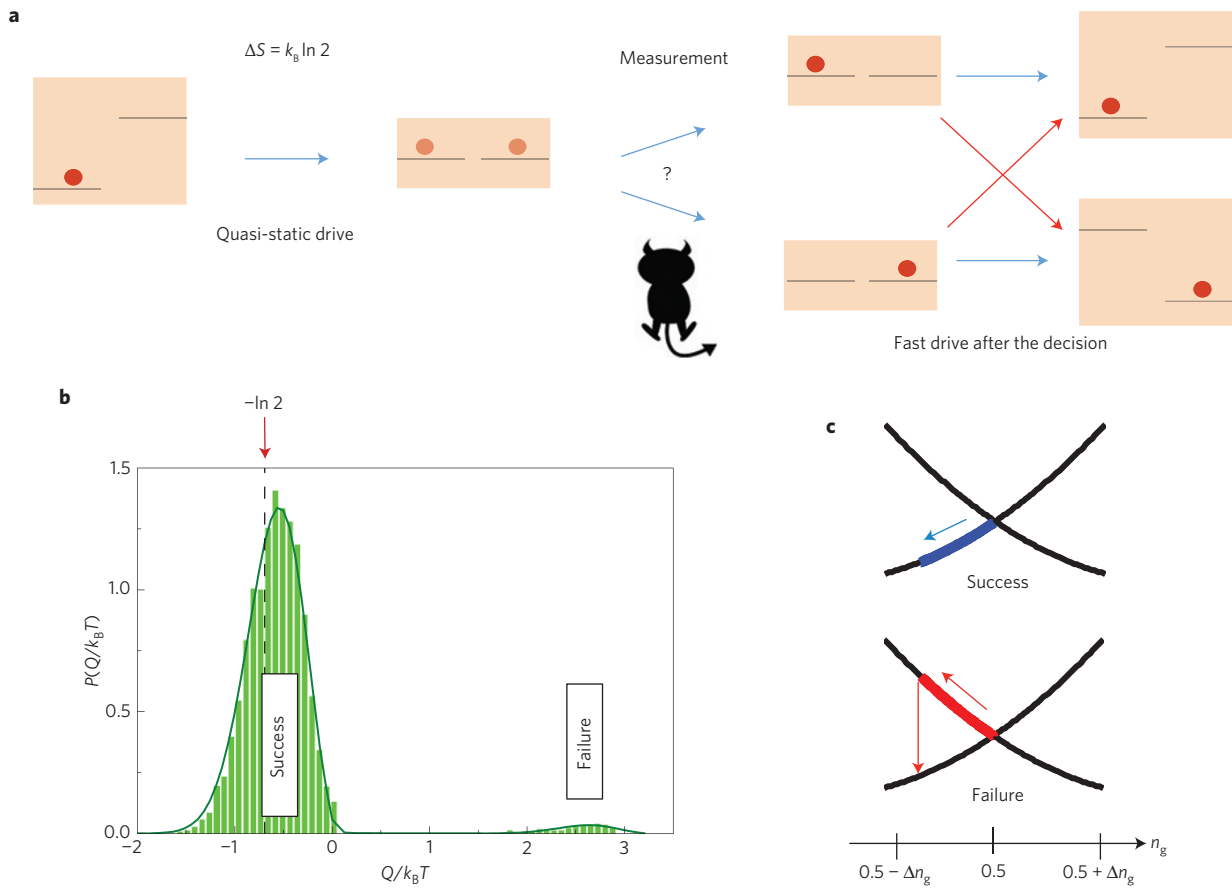


**Figure 4 | Experimental implementation of Maxwell's demon.** **a**, The principle and the protocol of the experiment on a single-electron box<sup>34</sup>. Initially, the two-level (in this case, classical) system is positioned such that the system is in one of the charge states. The control parameter  $n_g$  is then ramped quasi-statically to the degeneracy point, indicated by a change in the energy levels, from being largely unequal to fully equal. This leads to heat transport of  $k_B T \ln 2$  from the bath to the two-level system. Based on the outcome of the measurement by the Maxwell's demon of the state of the system (the conditional route in the text), the control parameter is quickly moved to one of the definite charge states. After this 'feedback' stage, the cycle repeats. **b**, The distribution of heat deposited in the bath,  $Q$ , based on about 3,000 cycles. The average heat extracted,  $\langle -Q \rangle$ , is about 75% of  $k_B T \ln 2$ . **c**, Illustration of how the histogram in **b** splits into two peaks. The two sections of parabolas in each case correspond to the positions of the energy levels in **a**. When  $n_g$  is moved quickly from  $1/2$  to  $1/2 - \Delta n_g$ , the state of the system can be  $n=0$  (success) or  $n=1$  (failure, with dissipation). Successful and unsuccessful fast ramps are also indicated on the right-hand side of **a** by the horizontal blue and crossing red arrows, respectively.

molecules<sup>2,3</sup>. In another experiment, more general fluctuation relations under time-dependent driving conditions were tested with the two islands in the SEB at unequal temperatures<sup>30</sup>. In the case with two baths, the Jarzynski equality fails naturally, but fluctuation relations based on trajectory entropy<sup>31</sup> and thermodynamic entropy recover equations (1) and (2).

**The role of information**

Information-to-energy conversion, embodied by Maxwell's demon, has recently become a topic of increased activity in nanosystems. One of the pioneering experiments in this field involved a microbead in an electric field<sup>32</sup>. Several proposals for nanoelectronic circuits have been put forward since then (see, for example, ref. 33). But experimentally, Maxwell's demon was realized in such a circuit only very recently<sup>34,35</sup>. Here we briefly discuss the principle of the demon, and the results of the experiments performed on an SEB (Fig. 4).

The aim of the experiment is to extract heat from a bath using information gathered by the SET detector, which senses the charge state of the SEB as in Fig. 3a. Initially, the driving field  $n_g$  is set to a value  $n_{g,0} = (1/2) - \Delta n_g$ , which is sufficiently far from the degeneracy value  $n_g = 1/2$  of the two charge states (equation (4)). At  $n_{g,0}$ , the SEB is almost certainly in one of the two charge states, and

owing to the symmetry of the Hamiltonian in equation (4),  $\Delta n_g > 0$  and  $n=0$  can be chosen without loss of generality. Thereafter,  $n_g$  is swept quasi-statically to  $n_g = 1/2$ . At this degeneracy point,  $n$  can take the value  $n=0$  or  $n=1$  with equal probability,  $p(n) = 1/2$ . This process thus increases the entropy of the charge system  $S = -k_B \sum_{n=0,1} p(n) \ln p(n)$  by  $\Delta S = k_B \ln 2$ . Because the process is quasi-static, this entropy change is equal to the decrease of entropy in the bath, and therefore the heat absorbed by the charge system from the electron bath is  $\Delta Q = T \Delta S = k_B T \ln 2$  in this ramp.

One might imagine completing such a cycle in many ways: either deterministically, without using the demon's information, or conditionally, depending on the outcome of the measurement—that is, by using the information. If the measurement and feedback were missing, as in the first, deterministic case, the average dissipation in the system would have been non-negative in repeated experiments. At best, one could move the driving field  $n_g$  quasi-statically back to the original position  $n_{g,0}$ , and inject the same heat  $k_B T \ln 2$  back into the bath. This process as a whole would then be reversible. The returning leg from the degeneracy point to the original position bears in this case a close relation to the Landauer principle of minimum heat  $k_B T \ln 2$  generated in the erasure of a bit<sup>36</sup>, which was recently demonstrated experimentally using a colloidal particle trapped in a modulated double-well potential<sup>37</sup>. On the other hand,



one could move  $n_g$  quickly back to the original position. Then, with some luck the system would be in the  $n = 0$  state at the moment of this abrupt change, and there would be no electron transitions and no heat exchange between the charge system and the bath. ‘Lucky’ here implies that the system happened to be in state  $n = 0$  at the moment of this quick change of the control parameter to  $n_g = n_{g,0}$ . In that case, one would have cooled the bath by  $k_B T \ln 2$  even after completing this closed cycle. But by gambling without knowing the actual value of  $n$  before the quick ramp, one is lucky only 50% of the time. And in the case that the system happened to be in the opposite state,  $n = 1$ , initially, it would make the  $n : 1 \rightarrow 0$  transition at  $n_g = n_{g,0}$  after the abrupt change, dissipating heat  $2E_C \Delta n_g$ , according to equation (4). This heat is much larger than  $k_B T$ , according to our initial premise that the  $n = 1$  state was very unlikely in equilibrium at this value of the driving field. Thus repeating such a cycle many times, one would inevitably inject heat to the bath. Owing to symmetry, the results above do not depend whether one moves to  $n_g = n_{g,0}$  or to  $n_g = 1 - n_{g,0}$  from the degeneracy point.

But it is precisely here that our demon comes to the rescue, in the second, conditional route for completing the cycle. Instead of deterministically jumping  $n_g : 1/2 \rightarrow n_{g,0}$  in each cycle, the demon measures the charge state at degeneracy and, based on the outcome of this measurement, the driving field is moved to  $n_{g,0}$  if  $n = 0$ , or to its symmetric point  $1 - n_{g,0}$  if  $n = 1$ . In both cases, one would successfully extract  $k_B T \ln 2$  in the whole cycle, if the measurement and feedback are error free. Being at  $n_g = n_{g,0}$  or  $n_g = 1 - n_{g,0}$ , one then starts another quasi-static ramp towards the degeneracy point, which makes the process cyclic and extracts ideally  $k_B T \ln 2$  heat from the bath in each round. This heat ends up in the detector circuit.

Figure 4b presents a typical outcome of a measurement, similar to those obtained in ref. 34. It is the histogram of heat dissipated into the bath in about 3,000 cycles. This histogram can be split into two main components: those cycles in which the demon has been successful, and the heat is  $Q \approx -k_B T \ln 2$ , and those in which the demon makes a mistake, and the heat dissipated is about  $+2E_C \Delta n_g$ . As long as the latter type of cycle is sufficiently rare, as in Fig. 4b, the average heat dissipated to the bath,  $Q_{\text{ave}}$ , is negative—the demon effectively cools the bath. For the measurement in Fig. 4b, we obtain  $Q_{\text{ave}} \approx -0.75 k_B T \ln 2$ , such that the fidelity of the demon is about 75%. The measurement thus represents a refrigerator of an electron gas, powered by information. The repetition frequency of the cycle at present is, however, far too slow to achieve observable cooling of the electron system in terms of a measurable temperature drop. In ref. 35, the influence of measurement errors of the demon were considered using the concept of mutual information  $I$ . The measurement on an SEB demonstrated that under the feedback conditions the histograms of the type shown in Fig. 4b are governed by the Sagawa–Ueda equality, which reads  $(e^{-\beta(W-\Delta F)-I}) = 1$  (ref. 38).

### Open questions and future directions

In most of the examples presented so far, quantum coherence effects do not play a role: the circuits operate essentially in the classical regime, apart from making use of quantum phenomena such as superconductivity and transport by tunnelling. It is often noted that the real challenge is to describe the dissipation in true quantum systems<sup>39–42</sup>. One way of putting it is that work is not an operator but instead a quantity that depends on a particular trajectory. The only ‘simple’ case is a closed quantum system that evolves in a unitary way<sup>39,40</sup>. Thus, if one could ‘measure the whole Universe’, then work could be determined as well. This is naturally not possible. Yet, in superconducting quantum circuits, for example, in qubits, it is possible to describe the system and its environment in a controlled way<sup>43,44</sup>. If one could then measure the system (qubit) and its environment, it would be at least a partial solution to the problem.

Suppose an on-chip resistive element is coupled to the superconducting quantum circuit in such a way that the energy relaxation of the system is taking place largely by photon exchange with this absorber<sup>45</sup>. A sensitive thermometer, at present being developed in several laboratories<sup>46–48</sup>, could then detect the temperature variations of the absorber that has minimal heat capacity. First estimates show that the present realizations are only about one order of magnitude away from single-photon resolution<sup>48</sup>. Such a measurement would be a major step forward, as the experiments described so far, apart from the measurements of average heat current<sup>8–10,12</sup>, rely on charge counting, rather than detecting the heat input directly. An alternative scheme might involve interferometric detection<sup>49,50</sup>, which could be applicable in circuit QED experiments<sup>51</sup>.

Where do we go from here? At this time, non-equilibrium fluctuation relations have not yet been probed in open quantum systems. Issues of incomplete measurements, non-Markovian systems and detector back-action in relation to fluctuation relations would be similarly interesting directions to take—and they can probably all be directly probed in superconducting or semiconducting circuits. A Brownian refrigerator, directly powered by thermal noise, is also an interesting concept yet to be demonstrated in experiment<sup>52,53</sup>.

Another relevant question is naturally: what is it all good for? Aside from purely satisfying our curiosity, studies of (quantum) non-equilibrium relations may prove useful in designing refrigerators and heat engines in which the role of fluctuations cannot be ignored. They may also help us to identify optimal driving schemes for maximizing work extraction or minimizing heat production in these devices<sup>1</sup>. Furthermore, Maxwell’s demon, although at present providing a very tiny power output, may in the future decrease dissipation locally with the help of feedback.

Received 4 August 2014; accepted 30 October 2014;  
published online 3 February 2015

### References

- Seifert, U. Stochastic thermodynamics, fluctuation theorems, and molecular machines. *Rep. Prog. Phys.* **75**, 126001 (2012).
- Aleman, A. & Ritort, F. Fluctuation theorems in small systems: Extending thermodynamics to the nanoscale. *Europhys. News* **41**, 27–30 (2010).
- Aleman, A., Ribezzi, M. & Ritort, F. in *Nonequilibrium Statistical Physics of Small Systems: Fluctuation Relations and Beyond* (eds Klages, R., Just, W. & Jarzynski, C.) (Wiley-VCH, 2012).
- Giazotto, F., Heikkilä, T. T., Luukanen, A., Savin, A. M. & Pekola, J. P. Opportunities for mesoscopics in thermometry and refrigeration: Physics and applications. *Rev. Mod. Phys.* **78**, 217–274 (2006).
- Courtois, H., Hekking, F. W. J., Nguyen, H. Q. & Winkelmann, C. Electronic coolers based on superconducting tunnel junctions: Fundamentals and applications. *J. Low Temp. Phys.* **175**, 799–812 (2014).
- Prance, J. R. *et al.* Electronic refrigeration of a two-dimensional electron gas. *Phys. Rev. Lett.* **102**, 146602 (2009).
- Pendry, J. B. Quantum limits to flow of information and entropy. *J. Phys. A* **16**, 21612171 (1983).
- Schwab, K., Henriksen, E. A., Worlock, J. M. & Roukes, M. L. Measurement of the quantum of thermal conductance. *Nature* **404**, 974–977 (2000).
- Meschke, M., Guichard, W. & Pekola, J. P. Single-mode heat conduction by photons. *Nature* **444**, 187–190 (2006).
- Timofeev, A. V., Helle, M., Meschke, M., Möttönen, M. & Pekola, J. P. Electronic refrigeration at the quantum limit. *Phys. Rev. Lett.* **102**, 200801 (2009).
- Ciliberto, S., Imparato, A., Naert, A. & Tanase, M. Heat flux and entropy produced by thermal fluctuations. *Phys. Rev. Lett.* **110**, 180601 (2013).
- Jezouin, S. *et al.* Quantum limit of heat flow across a single electronic channel. *Science* **342**, 601–604 (2013).
- Blanter, Y. M. & Büttiker, M. Shot noise in mesoscopic conductors. *Phys. Rep.* **336**, 1–166 (2000).
- Averin, D. V. & Pekola, J. P. Violation of the fluctuation-dissipation theorem in time-dependent mesoscopic heat transport. *Phys. Rev. Lett.* **104**, 220601 (2010).
- Sergi, D. Energy transport and fluctuations in small conductors. *Phys. Rev. B* **83**, 033401 (2011).
- Zhan, F., Denisov, S. & Hänggi, P. Power spectrum of electronic heat current fluctuations. *Phys. Status Solidi B* **250**, 2355–2364 (2013).

17. Evans, D. J., Cohen, E. G. D. & Morriss, G. P. Probability of second law violations in shearing steady states. *Phys. Rev. Lett.* **71**, 2401–2404 (1993).
18. Utsumi, Y. *et al.* Bidirectional single-electron counting and the fluctuation theorem. *Phys. Rev. B* **81**, 125331 (2010).
19. Küng, B. *et al.* Irreversibility on the level of single-electron tunneling. *Phys. Rev. X* **2**, 011001 (2012).
20. Cuetara, G. B., Esposito, M., Schaller, G. & Gaspard, P. Effective fluctuation theorems for electron transport in a double quantum dot coupled to a quantum point contact. *Phys. Rev. B* **88**, 115134 (2013).
21. Golubev, D. S., Utsumi, Y., Marthaler, M. & Schön, G. Fluctuation theorem for a double quantum dot coupled to a point-contact electrometer. *Phys. Rev. B* **84**, 075323 (2011).
22. Nakamura, S. *et al.* Nonequilibrium fluctuation relations in a quantum coherent conductor. *Phys. Rev. Lett.* **104**, 080602 (2010).
23. Jarzynski, C. Nonequilibrium equality for free energy differences. *Phys. Rev. Lett.* **78**, 2690–2693 (1997).
24. Crooks, G. E. Entropy production fluctuation theorem and the nonequilibrium work relation for free energy differences. *Phys. Rev. E* **60**, 2721–2726 (1999).
25. Büttiker, M. Zero-current persistent potential drop across small-capacitance Josephson junctions. *Phys. Rev. B* **36**, 3548–3555 (1987).
26. Averin, D. V. & Likharev, K. K. in *Mesoscopic Phenomena in Solids* (eds Altshuler, B. L., Lee, P. A. & Webb, R. A.) 173–271 (Elsevier, 1991).
27. Lafarge, P. *et al.* Direct observation of macroscopic charge quantization. *Z. Phys. B* **85**, 327–332 (1991).
28. Averin, D. V. & Pekola, J. P. Statistics of the dissipated energy in driven single-electron transitions. *Europhys. Lett.* **96**, 67004 (2011).
29. Saira, O.-P. *et al.* Test of Jarzynski and Crooks fluctuation relations in an electronic system. *Phys. Rev. Lett.* **109**, 180601 (2012).
30. Koski, J. V. *et al.* Distribution of entropy production in a single-electron box. *Nature Phys.* **9**, 644–648 (2013).
31. Seifert, U. Entropy production along a stochastic trajectory and an integral fluctuation theorem. *Phys. Rev. Lett.* **95**, 040602 (2005).
32. Toyabe, S., Sagawa, T., Ueda, M., Muneyuki, E. & Sano, M. Experimental demonstration of information-to-energy conversion and validation of the generalized Jarzynski equality. *Nature Phys.* **6**, 988–992 (2010).
33. Strasberg, P., Schaller, G., Brandes, T. & Esposito, M. Thermodynamics of a physical model implementing a Maxwell Demon. *Phys. Rev. Lett.* **110**, 040601 (2013).
34. Koski, J. V., Maisi, V. F., Pekola, J. P. & Averin, D. V. Experimental realization of a Szilard engine with a single electron. *Proc. Natl Acad. Sci. USA* **111**, 13786–13789 (2014).
35. Koski, J. V., Maisi, V. F., Sagawa, T. & Pekola, J. P. Experimental observation of the role of mutual information in the nonequilibrium dynamics of a Maxwell Demon. *Phys. Rev. Lett.* **113**, 030601 (2014).
36. Landauer, R. Irreversibility and heat generation in the computing process. *IBM Res. J. Dev.* **5**, 183–191 (1961).
37. Bérut, A. *et al.* Experimental verification of Landauer's principle linking information and thermodynamics. *Nature* **483**, 187–189 (2012).
38. Sagawa, T. & Ueda, M. Generalized Jarzynski equality under nonequilibrium feedback control. *Phys. Rev. Lett.* **104**, 090602 (2010).
39. Kurchan, J. A quantum fluctuation theorem. Preprint at <http://arxiv.org/abs/cond-mat/0007360> (2000).
40. Talkner, P., Lutz, E. & Hänggi, P. Fluctuation theorems: Work is not an observable. *Phys. Rev. E* **75**, 050102(R) (2007).
41. Esposito, M., Harbola, U. & Mukamel, S. Nonequilibrium fluctuations, fluctuation theorems, and counting statistics in quantum systems. *Rev. Mod. Phys.* **81**, 1665–1702 (2009).
42. Campisi, M., Hänggi, P. & Talkner, P. Colloquium: Quantum fluctuation relations: Foundations and applications. *Rev. Mod. Phys.* **83**, 771–791 (2011).
43. Makhlin, Y., Schön, G. & Shnirman, A. Quantum-state engineering with Josephson-junction devices. *Rev. Mod. Phys.* **73**, 357–400 (2001).
44. Clarke, J. & Wilhelm, F. K. Superconducting quantum bits. *Nature* **453**, 1031–1042 (2008).
45. Pekola, J. P., Solinas, P., Shnirman, A. & Averin, D. V. Calorimetric measurement of work in a quantum system. *New J. Phys.* **15**, 115006 (2013).
46. Schmidt, D. R., Yung, C. S. & Cleland, A. N. Nanoscale radio-frequency thermometry. *Appl. Phys. Lett.* **83**, 1002–1004 (2003).
47. Govenius, J. *et al.* Microwave nanobolometer based on proximity Josephson junctions. *Phys. Rev. B* **90**, 064505 (2014).
48. Gasparinetti, S. *et al.* Fast electron thermometry towards ultra-sensitive calorimetric detection. Preprint at <http://arxiv.org/abs/1405.7568> (2014).
49. Dorner, R. *et al.* Extracting quantum work statistics and fluctuation theorems by single-qubit interferometry. *Phys. Rev. Lett.* **110**, 230601 (2013).
50. Mazzola, L., Chiara, G. D. & Paternostro, M. Measuring the characteristic function of the work distribution. *Phys. Rev. Lett.* **110**, 230602 (2013).
51. Campisi, M., Blattmann, R., Kohler, S., Zueco, D. & Hänggi, P. Employing circuit QED to measure nonequilibrium work fluctuations. *New J. Phys.* **15**, 105028 (2013).
52. Van den Broeck, C. & Kawai, R. Brownian refrigerator. *Phys. Rev. Lett.* **96**, 210601 (2006).
53. Pekola, J. P. & Hekking, F. W. J. Normal-metal-superconductor tunnel junction as a brownian refrigerator. *Phys. Rev. Lett.* **98**, 210604 (2007).

## Acknowledgements

I thank J. Koski and M. Campisi for comments on the manuscript, and A. Feshchenko for providing illustration material. This work has been supported in part by the European Union Seventh Framework Programme INFERNOS (FP7/2007-2013) under grant agreement no. 308850, and by Academy of Finland (projects 250280 and 272218).

## Additional information

Reprints and permissions information is available online at [www.nature.com/reprints](http://www.nature.com/reprints).

## Competing financial interests

The author declares no competing financial interests.